Available online at www.sciencedirect.com
ScienceDirect
Atmospheric Environment 40 (2006) 6541–6553
ATMOSPHERIC ENVIRONMENT
www.elsevier.com/locate/atmosenv

On relationships between urban and rural near-surface meteorology for diffusion applications

Ashok K. Luhar[a,*], Akula Venkatram[b], Sang-Mi Lee[b]

[a]CSIRO Marine and Atmospheric Research, PMB 1, Aspendale, Vic. 3195, Australia
[b]Mechanical Engineering, University of California, Riverside, CA 92521, USA

Received 1 March 2006; received in revised form 23 May 2006; accepted 25 May 2006

Abstract

Dispersion of releases in urban areas can be estimated with information on micrometeorological variables in the urban boundary layer. However, this information is not generally available. On the other hand, meteorological measurements are routinely made in rural surroundings (e.g. airports). We examine empirical relationships between urban and rural meteorological variables using data from the Basel UrBan Boundary Layer Experiment (BUBBLE), conducted during June and July 2002 around Basel, Switzerland, and present two methods to estimate urban micrometeorology using measurements from rural sites. The first method is based on a two-dimensional internal boundary-layer model that uses rural variables as upwind inputs. It assumes that the urban Obukhov length is the same as that in the rural area in unstable conditions and that it is very large (neutral) in stable rural conditions. The second method uses a three-dimensional prognostic model called TAPM in which upwind rural observations are assimilated. Urban variables estimated from TAPM compare well with observations. This performance is slightly better than that of the internal boundary-layer model.

Keywords: Urban meteorology; Internal boundary layer; Urban–rural differences; TAPM; Urban dispersion; BUBBLE experiment

1. Introduction

Recent studies (Venkatram et al, 2005) indicate that simple dispersion models can be used to estimate ground-level concentrations in an urban area if meteorological information at the site is used to construct model inputs. Because such information is usually not available, there is a need for methods that can estimate urban meteorological variables from more routinely available rural measurements. This paper examines two such methods, one based on an analytical scheme for the height of the mechanical internal boundary layer coupled with Monin–Obukhov (M–O) surface similarity theory, and the other using a three-dimensional (3D) prognostic meteorological model. The performance of these two methods is evaluated with data from a boundary-layer field study conducted in the city of Basel, Switzerland, in 2002.

The urban boundary layer can generally be divided into four layers (e.g. Rotach et al., 2005): (1) the urban canopy layer that extends from the ground to about the average height of roughness elements (or buildings); (2) the roughness sublayer, displaying complex flows and extending to the height where the influence of the individual roughness elements

*Corresponding author. Tel.: +61 3 92394400; fax: +61 3 92394444.
E-mail address: ashok.luhar@csiro.au (A.K. Luhar).

1352-2310/$ - see front matter © 2006 Elsevier Ltd. All rights reserved.
doi:10.1016/j.atmosenv.2006.05.067

vanishes (roughly 2–5 times the height of typical roughness elements); (3) the inertial sublayer, equivalent to the surface layer over large, flat surfaces, where small-scale turbulence dominates transfer; and (4) the outer layer with mixing dominated by large-scale thermal effects. This paper focuses only on flow variables above the urban canopy layer. These variables govern the dispersion of releases at source–receptor distances at which the plume vertical extent is larger than the urban canopy height.

Before describing the models used to infer urban micrometeorology from rural inputs, we present analysis of the data used to evaluate these models.

2. Experimental data

The data analysed in this paper were collected as part of the Intensive Observation Period (IOP) 10 June–10 July 2002 of the Basel UrBan Boundary Layer Experiment (BUBBLE) conducted in the city of Basel, Switzerland (Rotach et al., 2005; http://pages.unibas.ch/geo/mcr/Projects/BUBBLE/). The BUBBLE measurements, both surface and upper air, were made using a number of instruments with the objective of studying boundary-layer and surface-exchange processes over different types of surfaces (i.e. urban, sub-urban and rural) and their role in the transport and diffusion of air pollution. This paper uses meteorological data from two towers.

The main urban measurements tower, Basel-Sperrstrasse (or U1), was 32 m high and located inside a street canyon in an area with dense, fairly homogeneous, residential building blocks, and a mean building height of 14.6 m AGL (above the ground level). In the vicinity of the measurement tower, the building height was 14 m AGL and the street canyon aspect ratio (i.e. height-to-width ratio) was about unity. The surface roughness length (z_0) was 2.1 m, and the zero-plane displacement height (d) was 9.5 m (Christen and Rotach, 2004). The tower measured the three wind components and temperature using sonic anemometers at six levels, viz. 3.6, 11.3, 14.7, 17.9, 22.4 and 31.7 m AGL, to characterise the vertical structure of the mean flow and turbulence within the urban roughness sub-layer (i.e. the layer directly influenced by individual roughness elements).

The rural site, Village Neuf (or R2), was located about 6.5 km NNW of the U1 site, and measured flow and turbulence at 3.3 m AGL over bare soil in an agricultural area ($z_0 = 0.07$ m). There are hills located south-east and north-east of the U1 (urban) site, generating drainage flow in the nighttime, but there is a relatively flat fetch to the north-west of the U1 site, within which the R2 (rural) site is located. 10-min averaged data on the mean temperature, mean wind components in the horizontal plane, standard deviations of the turbulent velocities in the three directions, cross-correlations of the turbulent velocities and sensible heat flux were available for both urban (at all heights) and rural areas, which were then averaged over hourly periods.

The BUBBLE data reveal the distinct influence of the urban surface on flow properties. This is examined next.

2.1. Observed winds

Fig. 1 shows wind roses at the six levels at U1, the urban tower. At the 31.7-m level (Fig. 1(a)), the wind is primarily from two sectors: 250°–360°, which mostly corresponds to daytime observations, and 90°–150°, which is dominated by nighttime and early morning hours (flows during these hours are influenced by drainage from the hills situated in the east, south-east of the monitoring site). The winds during the nocturnal hours are weaker than those in the daytime.

Fig. 1(b) for the 22.4-m level is similar to that for the 31.7-m level, with the main difference being an overall weakening of the winds at the lower height. In Fig. 1(c) for the 17.9-m level, the wind speeds decrease further, and the flow from the south-east quadrant has a larger easterly component. At 14.7 m (Fig. 1(d)), which is almost the local roof-top level, the winds become even lighter, with the dominant wind direction being east–north–east, which is also the direction of the local street. This behaviour suggests that the flow is now substantially influenced by the confining local street canyon. The dominant flow direction at the 11.3-m level (Fig. 1(e)), which lies within the street canyon, is along the direction of the street, with a small percentage of winds from the *northern* side of the street canyon.

In Fig. 1(e) for the 3.6-m level, the dominant flow is again along the direction of the street canyon; however, a small percentage of winds is from the *southern* side of the street canyon, which perhaps is in coherence with the flow from the *northern* side of the street canyon at 11.3 m but is in the opposite direction, possibly due to the formation of a cross-street vortex (e.g. Baik et al., 2000). The above wind roses suggest that the levels below 22.4 m are directly influenced by the local roughness elements.

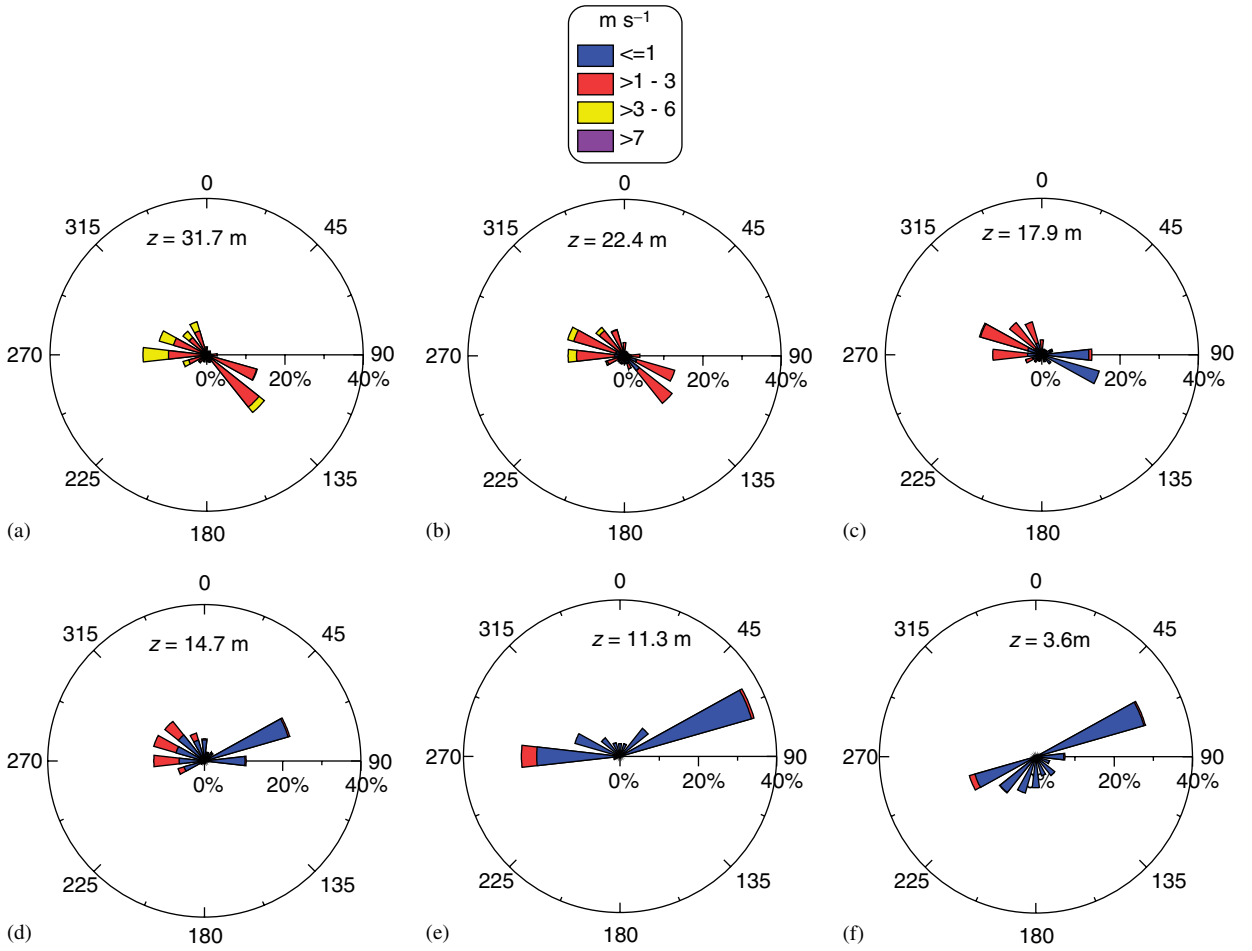

Fig. 1. Wind roses observed at six heights (AGL) at the Basel-Sperrstrasse urban monitoring site (U1) for the period 10 June–10 July 2002. The number of hourly-averaged observations is around 740 for each plot. The mean building height of the urban residential area is 14.6 m AGL.

A wind rose derived using the measurements made at 3.3 m AGL at the rural monitoring site R2 is shown in Fig. 2. It is found that the wind directions from the north-west quadrant, mostly occurring in the daytime, correlate well with those measured above the roof-top levels at the urban site; for example, the correlation (r) is 0.8 when compared with the wind vectors at 31.7 m. The winds from the sector 0°–120° occur largely at nighttime, and most probably correspond to light drainage flows from the local hills located on the eastern side of the monitoring station.

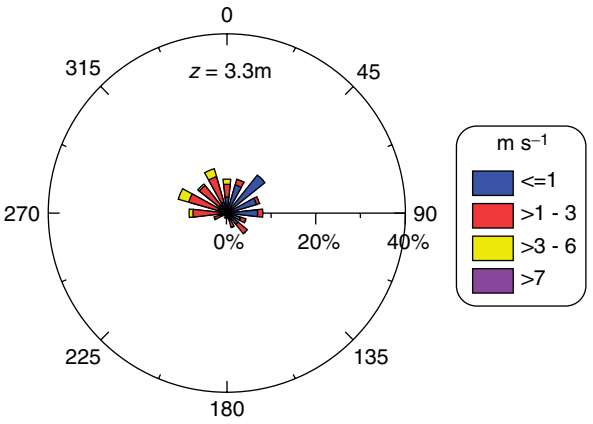

Fig. 2. Wind rose observed at 3.3 m AGL at the Village Neuf rural monitoring site (R2) for the period 10 June–10 July 2002. The number of hourly-averaged observations used is 698.

2.2. Surface similarity relations

The height of the roughness sublayer is low for densely built sites and high for low density areas.

There are no well-defined, quantitative definitions for calculating the height of the roughness sublayer. Christen and Rotach (2004) assume that it is the height that corresponds to the maximum Reynolds stress (or friction velocity), which for the BUBBLE data is the 22.4-m level.

M–O surface similarity for large, flat surfaces is expected to be valid within the inertial sublayer overlying the roughness sublayer. Thus, our analysis is confined to observations made at the 22.4 and 31.7-m levels. Also, we only consider those hours for which the rural wind direction is between 280° and 360° so that the urban area is downwind of the rural measurement site, a necessary configuration when investigating urban meteorology in terms of rural data. The sample size for each level is approximately 240, of which about 80% correspond to daytime, unstable conditions. The rest (20%) of the data, which correspond to the nighttime, are weakly unstable (or near neutral) at the urban site and stable at the rural site (see Section 2.3).

According to M–O similarity, the mean wind profile $U(z)$ in the diabatic surface layer is given as (e.g. van Ulden and Holtslag, 1985)

$$U(z) = \frac{u_*}{\kappa}\left[\ln\left(\frac{z-d}{z_0}\right) - \psi_m(\zeta_1) + \psi_m(\zeta_0)\right], \qquad (1)$$

where z is the height above the surface ($>d$), κ is the von-Karman constant ($=0.4$), u_* is the friction velocity, $\zeta_1 = (z-d)/L$, $\zeta_0 = z_0/L$, the function ψ_m is

$$\psi_m(\zeta) = 2\ln\left(\frac{1+x'}{2}\right) + \ln\left(\frac{1+x'^2}{2}\right) - 2\tan^{-1}(x') + \frac{\pi}{2} \quad \text{for } L<0, \qquad (2)$$

$$\psi_m(\zeta) = -17[1-\exp(-0.29\zeta)] \quad \text{for } L\geqslant 0, \qquad (3)$$

L is the Obukhov length, and $x' = (1-16\zeta)^{1/4}$. The similarity relation (1) coupled with Eq. (2) in unstable conditions can be applied to heights greater than $|L|$, even though, strictly speaking, they are valid for smaller heights. Similarly, Eq. (3) for stable conditions, in addition to being applicable for $z<L$, can also be used for $z>L$ with good accuracy (van Ulden and Holtslag, 1985). The values of all the parameters used in the above equations are available, or can be derived, from the BUBBLE measurements. The values of u_* and L observed at 22.4 m were used in the above similarity relations.

A comparison of the wind speeds estimated using Eq. (1) with the observed data at 31.7 m in Fig. 3(a) shows that M–O surface similarity performs well at describing the data, although there is a tendency for it to overestimate. This overestimation increases for the 22.4-m level (Fig. 3(b)), coupled with a slight increase in the scatter of the points. Departure from the similarity behaviour is expected as the measurement level decreases towards the height of

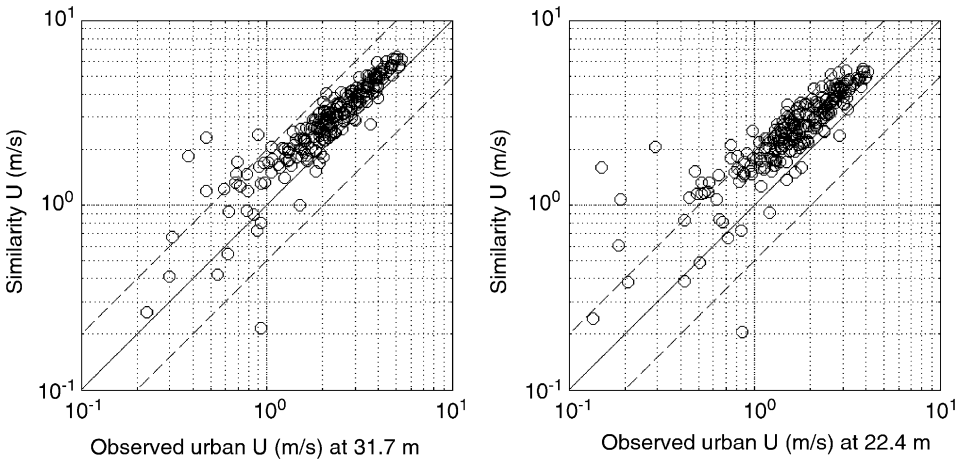

Fig. 3. Scatter plots of the wind speeds estimated using M–O similarity vs. the observed wind speeds at two levels over the urban area. The solid line is the perfect-fit line and the dashed lines are the factor-of-two lines.

the roughness element. It is possible that even the 31.7 and 22.4-m levels are well within the influence of the roughness sublayer. Consequently, M–O similarity may be valid only approximately for these two levels (it is expected that for heights greater than 31.7 m in the surface layer, M–O similarity should perform better).

In the surface layer, a similarity parameterisation for the standard deviation of the vertical turbulent velocity (σ_w), which is a controlling parameter in the vertical diffusion of a contaminant plume, is (Panofsky et al., 1977)

$$\sigma_w = c_1 u_* \left(1 - 3\frac{(z-d)}{L}\right)^{1/3} \quad \text{for } L<0, \tag{4}$$

$$\sigma_w = c_1 u_* \quad \text{for } L \geqslant 0, \tag{5}$$

where the value of the regression constant c_1 is still uncertain. Panofsky et al. use $c_1 = 1.3$, Savelyev and Taylor (2005) use 1.25, and Stull (1988) gives a range of 1–1.6. In Fig. 4, the values of σ_w calculated using Eqs. (4) and (5) with $c_1 = 1.1$ and the observed u_* and L for the 31.7 and 22.4-m levels are plotted against the measurements. These plots show the similarity Eqs. (4) and (5) provide an adequate description of the data.

The above comparison plots all involve weakly unstable (or near-neutral) to unstable conditions since stable conditions were not encountered at the urban site in the nighttime. The similarity relationships (1)–(5) also describe the measurements at the rural site R2 well (plots not shown). We use these functional relationships in Section 3.

2.3. Sensible heat flux

Fig. 5 compares the kinematic sensible heat fluxes observed at the two urban measurement levels with that measured at the rural site when the rural conditions are unstable (i.e. positive heat flux, daytime conditions). The daytime fluxes are well correlated, with the urban heat flux being almost twice as large as the rural heat flux. Overall, the heat flux at 31.7 m is slightly smaller than that at 22.4 m. The heat flux decreases with decreasing height in the street canyon (plots not shown), with the mid-day values in the street canyon becoming as low as half the rural values.

Fig. 6 is the same as Fig. 5, except when the rural conditions are stable (i.e. negative heat flux, nighttime conditions). There is no definite trend in the urban heat flux as a function of the rural values, but a noteworthy feature is that even though the rural stability is stable, the urban stability is always neutral or weakly unstable, a consequence of the thermal properties of the urban surface and the likely presence of an anthropogenic heat flux. We assume that the heat flux data at 22.4 m represent the surface heat flux over the urban area under study.

The magnitude of the friction velocity observed at the levels above the urban street canyon is almost twice as large as that over the rural area (plots not shown).

3. Estimating urban dispersion meteorology from rural values

In this section, we formulate a simple scheme to estimate urban meteorological parameters in terms

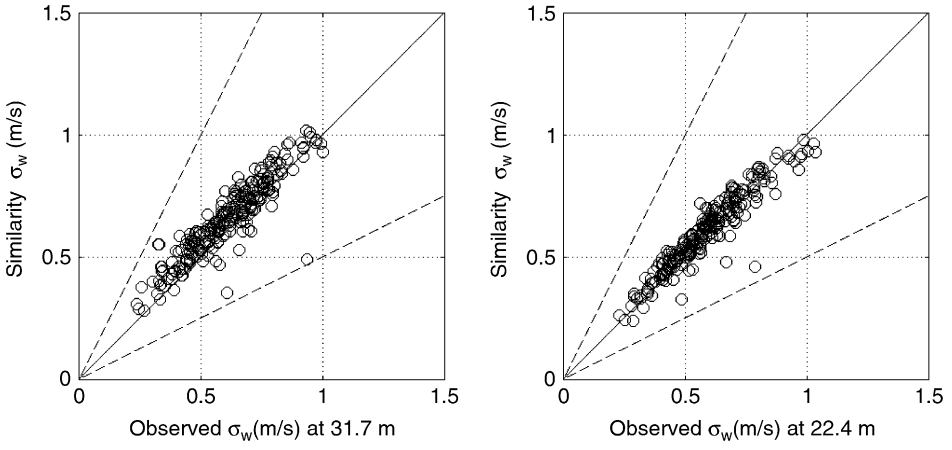

Fig. 4. Scatter plots of the standard deviation of the vertical turbulent velocity (σ_w) estimated using M–O similarity vs. the observed values at two heights over the urban area. The solid line is the perfect-fit line and the dashed lines are the factor-of-two lines.

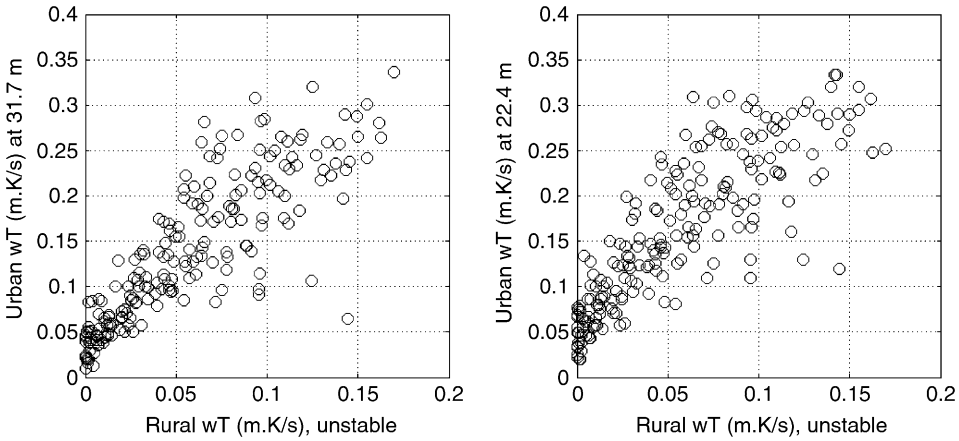

Fig. 5. Plots of the observed urban kinematic sensible heat flux vs. the observed rural kinematic sensible heat flux for two urban measurement levels when the rural conditions are unstable ($L_R<0$).

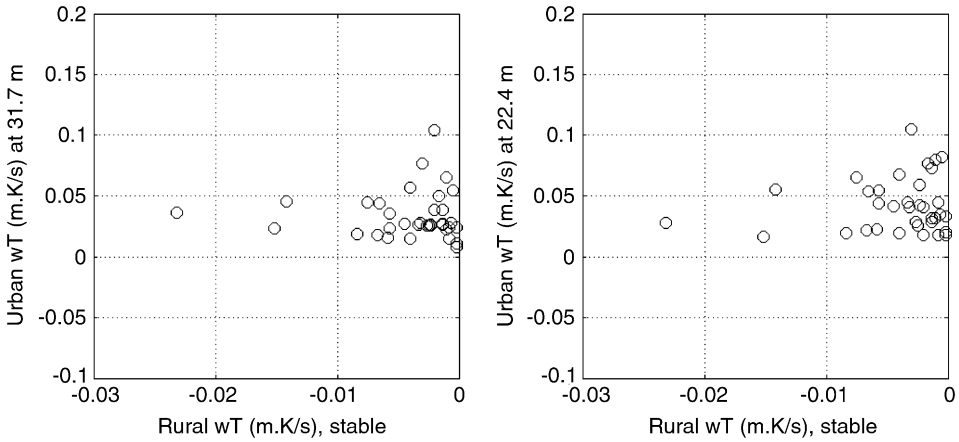

Fig. 6. Plots of the observed urban kinematic sensible heat flux vs. the observed rural kinematic sensible heat flux for two measurement levels when the rural conditions are stable ($L_R>0$).

of rural observations, and compare them with the BUBBLE data.

An internal boundary layer (IBL) is formed when air flows over a change in surface conditions such as surface roughness, thermal and moisture properties. We are interested in the IBL formed over an urban area due to a change in surface roughness and heat flux. There are a number of formulae of varying complexity to estimate the growth of the IBL (see Garratt, 1990; Savelyev and Taylor, 2005). One such formula based on Miyake's diffusion analogy and discussed by Savelyev and Taylor (2005) is

$$U(h)\frac{\mathrm{d}h}{\mathrm{d}x} = A\sigma_w, \tag{6}$$

where h is the height of the IBL, x is the downwind distance from the roughness change, $U(h)$ is the wind speed at height h, and A is a constant (≈ 1). We consider the values of $U(h)$ and σ_w to be those of the modified flow over the urban surface. The slowing of the mean wind over the urban surface after a step change in surface roughness will result in an upward mean velocity in order to satisfy continuity constraints. This upward velocity is neglected in Eq. (6).

We assume that M–O surface similarity theory is valid within the IBL over an urban area; the similarity comparisons presented earlier provide support for this assumption. We substitute the U and σ_w expressions from Eqs. (1), (4) and (5) at

$z = h$ into Eq. (6). Note that u_* cancels out; however L for the urban area needs to be specified, and is approximated using the assumptions given in the following paragraphs.

We assume that under the daytime convective mixing (i.e. unstable) conditions, L_U is the same as L_R (the subscripts R and U represent rural and urban, respectively). This assumption can be justified on the grounds that the sensible heat flux from an urban surface is usually greater than that from a rural area (as shown earlier for the BUBBLE data), and this increase in the sensible heat flux tends to compensate for the increase in the friction velocity over the urban surface in the calculation of L_U. When rural conditions are stable in the nighttime (i.e. $L_R > 0$), the heat flux comparison plot presented earlier shows that it is reasonable to assume that the conditions over the urban area are largely neutral (see also Britter and Hanna, 2003).

These assumptions about the M–O length over the urban area allow us to estimate the internal boundary-layer height h as a function of x from Eq. (6). We used a 4^{th}-order Runge–Kutta scheme to integrate the equation numerically to calculate h at distance $x = 5$ km, which is approximately the distance of the urban site from the outer edges of the urban built-up area located towards the direction of the rural site. Once h is known, the micrometeorological variables over the urban area can be calculated using two assumptions: (1) the micrometeorological variables above h are the same over the urban and the rural areas; and (2) the urban profiles below h follow M–O similarity.

By equating the rural and the urban wind speeds at $z = h$, we obtain the following expression for the urban friction velocity

$$u_{*,U} = u_{*,R} \frac{\ln\left(\frac{h-d_R}{z_{0,R}}\right) - \psi_m\left(\frac{h-d_R}{L_R}\right) + \psi_m\left(\frac{z_{0,R}}{L_R}\right)}{\ln\left(\frac{h-d_U}{z_{0,U}}\right) - \psi_m\left(\frac{h-d_U}{L_U}\right) + \psi_m\left(\frac{z_{0,U}}{L_U}\right)}. \quad (7)$$

As indicated earlier, we take $L_U = L_R$, when $L_R < 0$, and L_U is infinity when $L_R > 0$. We assume that for rural conditions $d_R = 0$.

Knowledge of $u_{*,U}$ allows us to calculate the wind speed profile within the IBL over the urban area. Section 3.1 compares these estimates of micrometeorological variables at a height of 22.4 m with corresponding observations.

3.1. Results from the analytical scheme

Fig. 7(a) compares estimates of u_* at 22.4 m from the IBL model to observed values over the urban area. The results suggest that the scheme tends to underestimate the observations, but its overall performance is good, given its simplicity: 85% of the model estimates lie within a factor of two of the observations, the correlation coefficient (r) is 0.62, and the slope and intercept of the linear regression line are 0.73 and 0.04 m s^{-1}, respectively.

In Fig. 7(b), we compare wind speeds computed with Eq. (1) and estimates of urban u_* obtained from the IBL model with observed wind speeds (U) at 22.4 m. We find that 77% of the model values are within a factor of two of the observations, r is 0.49, and the slope and intercept of the regression line are 0.76 and 0.73 m s^{-1}, respectively.

Fig. 7(c) compares estimates of σ_w from Eqs. (4) and (5), using the estimates of urban u_* obtained from the analytical scheme, with corresponding observations. The comparison indicates that 93% of the model values are within a factor of two of the observations, r is 0.56, and the slope and intercept of the regression line are 0.79 and 0.15 m s^{-1}, respectively.

The performance of the analytical scheme in estimating U and σ_w at the 31.7-m level is very similar to that for the 22.4-m level presented above (plots not shown).

Fig. 8(a) is the same as Fig. 7(a) except that only those hours for which the rural conditions are unstable have been considered. Although the correlation is good ($r = 0.74$), there is an overall underprediction of the observed u_*, very similar to that in Fig. 7(a). The plot in Fig. 8(b) corresponds to stable rural conditions, for which the sample size is much smaller, only 40 compared to 204 for the unstable conditions. The correlation coefficient is 0.56, and a tendency by the model to overpredict is evident.

Section 4 presents a comparison of estimates of micrometeorological variables from a numerical model with corresponding observations.

4. Numerical modelling

4.1. Model used

A mesoscale model called TAPM, which is a three-dimensional prognostic meteorological and

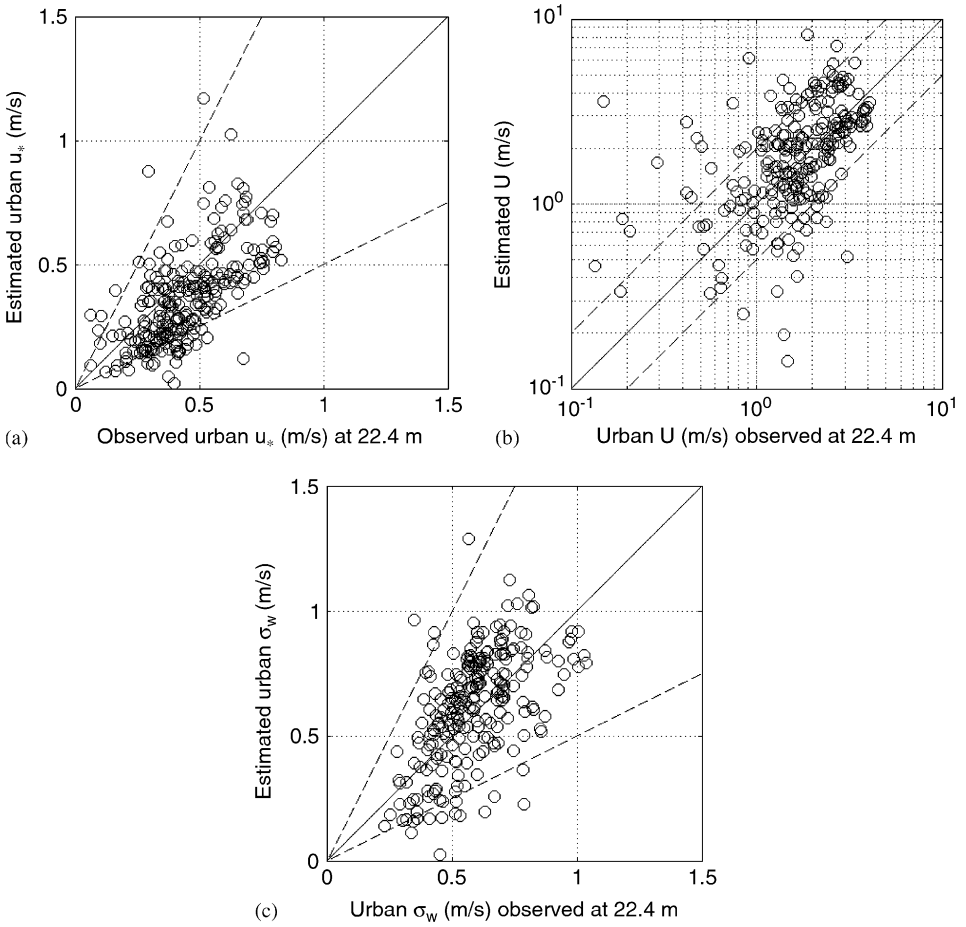

Fig. 7. Scatter plot of the data measured at 22.4 m over the urban area vs. the values computed from the present analytical scheme for (a) friction velocity (u_*), (b) wind speed (U), and (c) standard deviation of the vertical turbulent velocity (σ_w). The solid line is the perfect-fit line and the dashed lines are the factor-of-two lines.

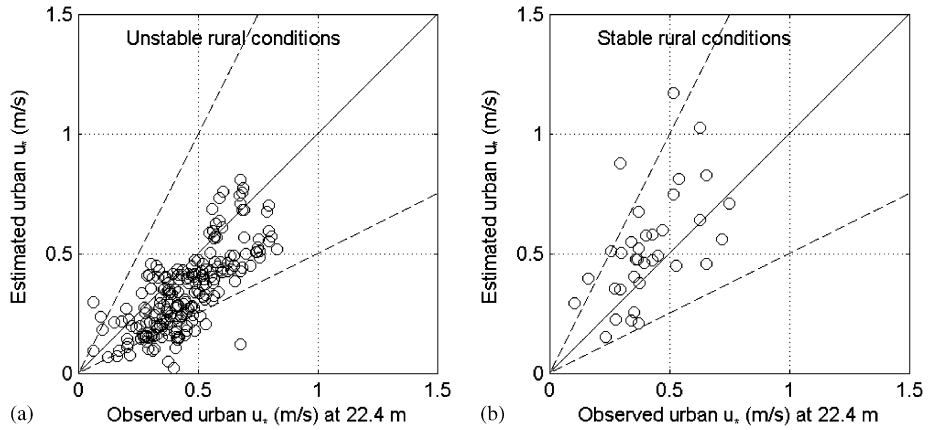

Fig. 8. Scatter plot of the observed u_* values at 22.4 m over the urban area vs. the values computed from the present analytical scheme for (a) unstable conditions (i.e. when the observed rural Obukhov length is <0), and (b) stable conditions (i.e. when the observed rural Obukhov length is >0). The solid line is the perfect-fit line and the dashed lines are the factor-of-two lines.

air pollution model, is used here to study the evolution of the flow from the rural to the urban area during the period 10 June–10 July 2002 of the BUBBLE experiment. Model details are given in Hurley (2005) and Hurley et al. (2005) (see also http://www.dar.csiro.au/tapm/), and some of the model validation studies conducted using TAPM are given in Hurley et al. (2003) and Luhar and Hurley (2003).

The meteorological component of TAPM solves the momentum equations for horizontal wind components, the incompressible continuity equation for the vertical velocity in a terrain-following coordinate system, and the scalar equations for potential virtual temperature, specific humidity of water vapour, cloud water and rain water. Wind observations can be optionally assimilated into the momentum equations as nudging terms.

Pressure is determined from the sum of hydrostatic and optional (not used here) non-hydrostatic components, and a Poisson equation is solved for the non-hydrostatic component. The model incorporates explicit cloud microphysical processes.

The turbulence closure terms in the mean equations use a gradient diffusion approach, including a counter-gradient term for the heat flux, with eddy diffusivity determined using prognostic equations for turbulence kinetic energy and eddy dissipation rate. A weighted vegetative canopy, soil and urban land-use scheme is used to predict energy partitioning at the surface, while radiative fluxes, both at the surface and at upper levels, are also included. Boundary conditions for the turbulent fluxes are determined by M–O surface-layer scaling variables and parameterisations for stomatal resistance. The turbulence levels in TAPM are determined directly by solving equations for turbulent kinetic energy and eddy dissipation rate.

The large-scale, three-dimensional synoptic meteorological fields of horizontal wind components, temperature and moisture, which are required as input boundary conditions in TAPM, are typically obtained from the Australian Bureau of Meteorology's GASP (Global AnalySis and Prediction) analyses, at a horizontal grid spacing of 1° (approximately 100 km) at 6-hourly intervals. The vertical levels of the input synoptic analyses are in a pressure coordinate system scaled by the surface pressure. The total of number of these levels is 29, of which the lowest ten are 0.991, 0.975, 0.95, 0.925, 0.9, 0.875, 0.85, 0.8, 0.75 and 0.7, and the highest is 0.01. Other inputs to the model include global databases of terrain height, land use, and monthly sea-surface temperature, given at approximate resolutions of 1, 1 and 100 km, respectively. For the study area, the soil type is assumed to be sandy clay loam.

Given the large-scale meteorology, TAPM simulates local scales at a finer resolution using a one-way multiple nesting approach, predicting local-scale meteorology, typically down to a resolution of 1 km, such as sea breezes and terrain induced flows.

4.2. Model setup

TAPM (version 3.0) was run with four nested grid domains at 20, 7.5, 2, 0.5 km resolution for meteorology (35×35 grid points), all centred at the location (7°36′E, 47°34′S), which is equivalent to 612.144 km east and 268.452 km north in the CH1903 geographic coordinate system used in Switzerland, and is almost the location of the U1 urban monitoring site. The lowest ten of the 25 vertical levels were 10, 25, 50, 100, 150, 200, 250, 300, 400 and 500 m AGL, with the highest model level at 8000 m AGL. The terrain height within the innermost model domain varies from 240 to 660 m above mean sea level.

Another input to the model is the deep soil volumetric moisture content (at a depth of about 1 m from the surface), which affects thermal properties of soil, thereby influencing the surface energy balance, and the micrometeorology of an area through the lower boundary condition in the model. Apart from an area being wetter, a higher value of the deep soil moisture content may also mean that the soil is more of clay type than sandy. A value of $0.2\,m^3\,m^{-3}$ was used for this parameter in the current study.

4.3. Land-use specification in the model

Parameters to specify land use and other ground-surface properties, such as soil type, are important inputs to the surface energy balance scheme of the model for calculating surface fluxes of heat and momentum. The lowest vertical level of the atmospheric domain (i.e. 10 m AGL) in TAPM is parameterised in terms of M–O surface similarity laws.

The land-surface scheme in TAPM calculates surface moisture, surface temperature and surface fluxes for bare soil, vegetation cover, and urban cover separately, and then uses a weighting scheme according to the fraction of the area covered by the three surfaces in order to derive the effective surface

values of these parameters. These surface values impose the lower boundary conditions in the model. The land-surface scheme in TAPM is in effect a single layer scheme, and therefore, does not resolve the flow within the urban or vegetation canopy. In the model there are a total of 40 land-use categories, of which 5 relate to urban land use. The most appropriate urban category for the urban area under study is Urban (high) (Category 34), which assumes that the fraction of the urban cover is 0.8 (high density), albedo is 0.13, the urban anthropogenic heat flux is 40 $W m^{-2}$, and the overall urban roughness length is 0.8 m (the model does not account for the zero-plane displacement height). Within the innermost model domain, the central urban (high) area is surrounded by pasture—mid-dense (seasonal), with patches of forest—low sparse (woodland), forest—mid-dense, grassland—mid-dense tussock, and pasture/herb-field—very sparse.

4.4. Wind data assimilation

In TAPM, wind observations are optionally assimilated into the momentum equations as nudging terms. The nudging is time dependent: it forces the model towards observed values at every time step, more when the observations are current and less at earlier and later times. Observations at any height can be included, and the observations can influence a user-specified number of model levels and horizontal radius for each site.

Keeping in view the aim of the present study, which is to estimate the surface-layer meteorology over an urban area given the upwind rural meteorology, we assimilated the wind speeds and wind directions observed at 3.3 m at the rural site R2 in TAPM while allowing the model to adjust these winds over the urban area. Model estimates of urban meteorological variables are compared with corresponding observations made at the urban site U1. In this way, the TAPM setup is also consistent with the IBL model used earlier in which observed rural meteorology is used as input. The observed rural wind speeds were extrapolated to the lowest six model levels using the following similarity relationship:

$$U(z) = U(z_1)\left[\ln\left(\frac{z}{z_0}\right) - \psi_m\left(\frac{z}{L_R}\right)\right] \Big/ \left[\ln\left(\frac{z_1}{z_0}\right) - \psi_m\left(\frac{z_1}{L_R}\right)\right], \quad (8)$$

where the rural measurement height $z_1 = 3.3$ m.

The extrapolated values were then assimilated into the model assuming that the wind direction was the same at all six levels. The assimilation scheme uses a radius of influence, within which the influence of a measurement decreases as the inverse of the square of distance from the measurement point. This radius was taken to be 15 km, which is large enough to allow the assimilated observations to influence the nocturnal drainage flow from the hills located south-east and north-east of the U1 site. However, such effects are likely to be unimportant for the hours chosen for analysis in this study. To make sure that the urban site was downwind of the rural measurement site, we selected only those hours when the rural wind direction was within 280°–360°.

4.5. TAPM results

The scatter plot in Fig. 9(a) compares TAPM predicted u_* with the observations at the rural site R2. Note that most of the observations correspond to unstable conditions. The model performance is very good, mainly because the observed winds at R2 have been assimilated into the model. Fig. 9(b) shows that the model is able to simulate u_* at the urban site U1 (at 22.4 m) well ($r = 0.69$); however, some bias for the model to underpredict is evident. The model u_* values at U1 are almost twice as high as those at R2, which is consistent with observed behaviour. Fig. 9(c) indicates that the model wind speeds at U1 are somewhat higher than the data, but their correlation with the observations is good ($r = 0.71$). The model predicted wind speeds at R2 (plot not shown) are almost the same as the data because of data assimilation.

Unlike the internal boundary-layer scheme presented earlier, TAPM can estimate heat fluxes in the rural and the urban areas considered here. The model predicted sensible heat flux at R2 is in agreement with the observations (Fig. 10(a)), but it is apparent that the magnitudes of lowest (negative) values are overestimated by the model. The comparison for the urban heat flux in Fig. 10(b) suggests that TAPM overpredicts the data, and that there are some negative model values for which the observed values are positive. In Fig. 10(b), the correlation is slightly better than that at the rural site. One reason for the scatter in Fig. 10(a) and Fig. 10(b) may be that the model is not predicting the clouds and their effects properly. The higher scatter in the latter figure also suggests

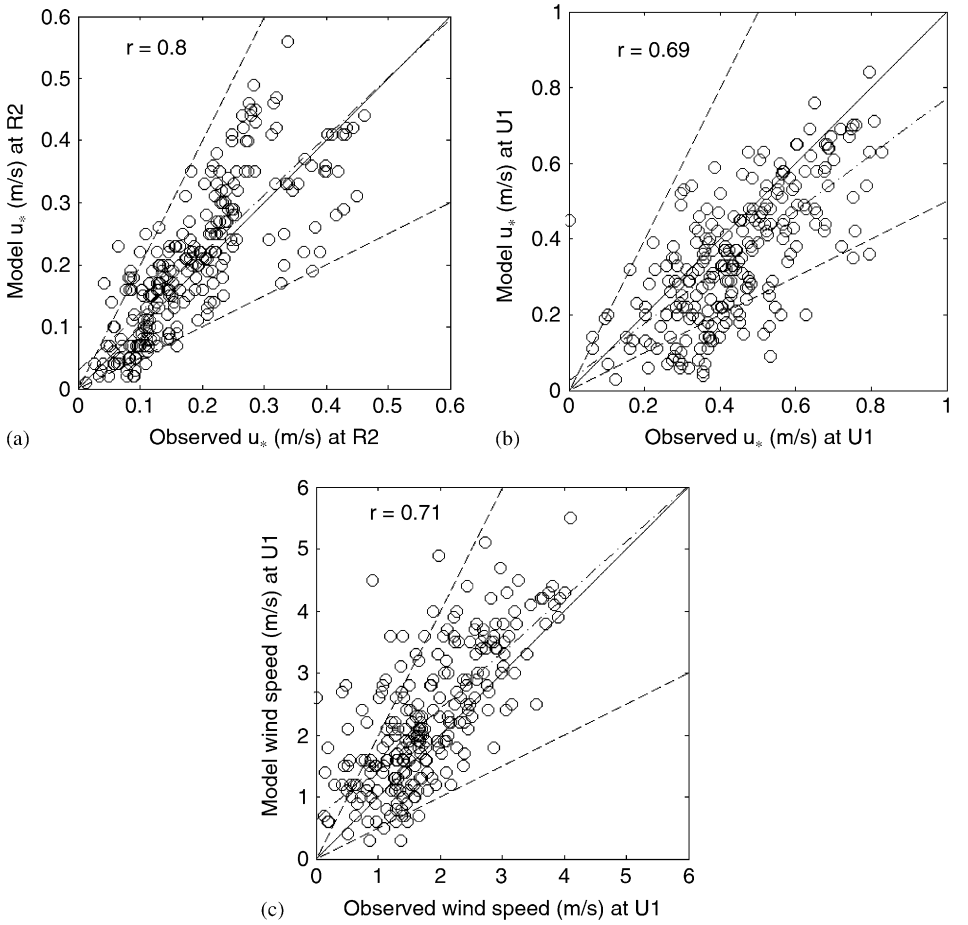

Fig. 9. Scatter plot of the TAPM-predicted u_* values vs. the data at (a) R2—rural site, and (b) U1—urban site; (c) scatter plot of the TAPM-predicted wind speeds vs. the data at U1. The solid line is the line of perfect fit, the dashed lines are the factor-of-two lines, and the dash-dot line is the best fit line.

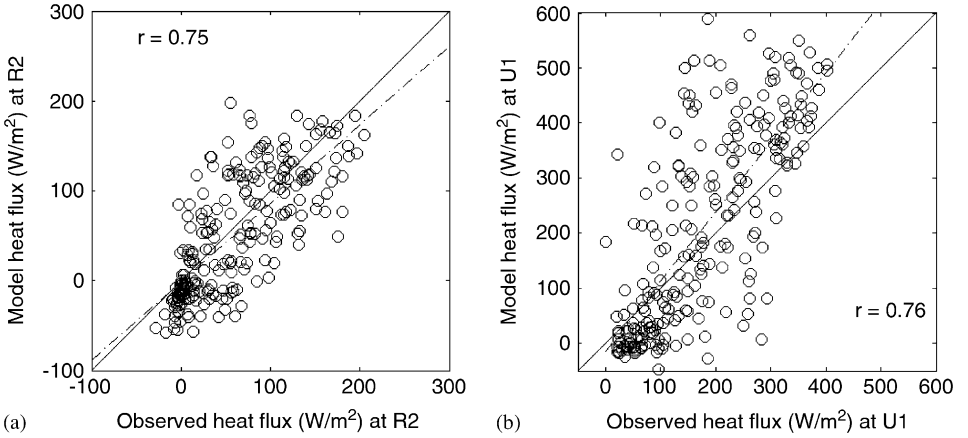

Fig. 10. Scatter plot of the TAPM-predicted vs. observed sensible heat flux at (a) R2—rural site, and (b) U1—urban site (at 22.4 m). The solid line is the line of perfect fit and the dash-dot line is the best fit line.

that a single layer urban land-surface scheme as used in TAPM is perhaps not an adequate description of the type of urban canopy considered in this paper.

5. Conclusions

The paper examines two methods to estimate micrometeorology over urban areas using measurements from rural sites. The work was motivated by the need to estimate dispersion in urban areas using rural meteorological inputs. The first method is based on a two-dimensional internal boundary-layer model that uses Monin–Obukhov surface similarity theory and rural variables as upwind inputs. The model assumes that the urban Obukhov length is the same as that in the rural area under unstable conditions and is infinity (neutral) when rural conditions are stable. The second method to compute urban variables uses a 3D prognostic model, CSIRO's TAPM, in which upwind rural observations are assimilated.

Results from these methods were compared with data from the Basel UrBan Boundary Layer Experiment (BUBBLE), conducted during June and July 2002 in the city of Basel, Switzerland. Estimates of friction velocity, winds, and turbulence estimated from both methods compared reasonably well with the observations. The performance of TAPM was slightly better than that of the internal boundary-layer model.

Characteristics of urban areas that can affect flow properties include roughness length, building characteristics, thermal properties of the surface and anthropogenic heat flux. Although TAPM accounts for these effects with a varying degree of complexity, the land-surface scheme in the model needs improvement to resolve the urban canopy layer and the roughness sublayer.

The internal boundary-layer (IBL) scheme incorporates the effects of the urban roughness length and, to a limited extent, those of thermal properties of the surface and anthropogenic heat flux by assuming a neutral stability in the nighttime. Although this scheme yields results that compare well with observations, it cannot estimate the urban heat flux when rural conditions are stable. This deficiency needs to be addressed because the urban heat flux controls the height of the (weakly) convective boundary layer that forms when the rural flow is stable. Because it is not practical to use TAPM in routine dispersion applications, the much simpler IBL scheme needs to be improved to allow estimation of urban heat fluxes.

Acknowledgements

The authors are grateful to Drs. S.-E. Gryning, M.W. Rotach, A. Christen, and others involved in the BUBBLE experiment for sharing the valuable data. This work was done while the first author was a visiting researcher at the University of California at Riverside. A. Venkatram's research was partially supported by the National Science Foundation through Grant ATMOS 0430776. Comments by an anonymous reviewer helped in improving the clarity of the paper.

References

Baik, J.-J., Park, R.-S., Chun, H.-Y., Kim, J.-J., 2000. A laboratory model of urban street-canyon flows. Journal of Applied Meteorology 39, 1592–1600.

Britter, R.E., Hanna, S.R., 2003. Flow and dispersion in urban areas. Annual Review of Fluid Mechanics 35, 469–496.

Christen, A., Rotach, M.W., 2004. Estimating wind speed at an urban reference height. Fifth AMS Symposium on the Urban Environment, 23–27 August, Vancouver, BC, Canada.

Garratt, J.R., 1990. The internal boundary layer—a review. Boundary-Layer Meteorology 50, 171–203.

Hurley, P., 2005. The Air Pollution Model (TAPM) Version 3. Part 1. Technical description. Australia. CSIRO Atmospheric Research. Technical Paper No. 71, 54pp., http://www.dar.csiro.au/tapm/.

Hurley, P., Manins, P., Lee, S., Boyle, R., Ng, Y., Dewundege, P., 2003. Year-long, high-resolution, urban airshed modelling: verification of TAPM predictions of smog and particles in Melbourne, Australia. Atmospheric Environment 37, 1899–1910.

Hurley, P.J., Physick, W.L., Luhar, A.K., 2005. TAPM: a practical approach to prognostic meteorological and air pollution modelling. Environmental Modelling and Software 20, 737–752.

Luhar, A.K., Hurley, P.J., 2003. Evaluation of TAPM, a prognostic meteorological and air pollution model, using urban and rural point-source data. Atmospheric Environment 37, 2795–2810.

Panofsky, H.A., Tennekes, H., Lenschow, D.H., Wyngaard, J.C., 1977. The characteristics of turbulent velocity components in the surface layer under convective conditions. Boundary-Layer Meteorology 11, 355–361.

Rotach, M.W., Vogt, R., Bernhofer, C., Batchvarova, E., Christen, A., Clappier, A., Feddersen, B., Gryning, S.-E., Martucci, G., Mayer, H., Mitev, V., Oke, T.R., Parlow, E., Richner, H., Roth, M., Roulet, Y.-A., Ruffieux, D., Salmond, J.A., Schatzmann, M., Voogt, J.A., 2005. BUBBLE—an

Urban Boundary Layer Meteorology Project. Theoretical and Applied Climatology 81, 231–261.

Savelyev, S.A., Taylor, P.A., 2005. Internal boundary layers: I. Height formulae for neutral and diabatic flows. Boundary-Layer Meteorology 115, 1–25.

Stull, R.B., 1988. An Introduction to Boundary Layer Meteorology. Kluwer Academic Publishers, Dordrecht, 666pp.

Van Ulden, A.P., Holtslag, A.A.M., 1985. Estimation of atmospheric boundary layer parameters for diffusion applications. Journal of Climate and Applied Meteorology 24, 1196–1207.

Venkatram, A., Isakov, V., Pankratz, D., Yuan, J., 2005. Relating plume spread to meteorology and urban areas. Atmospheric Environment 39, 371–380.